ASTRONOMY & ASTROPHYSICS
SUPPLEMENT SERIES
Astron. Astrophys. Suppl. Ser. **110**, 553-564 (1995)

The determination of T_{eff} of B, A and F main sequence stars from the continuum between 3200 Å and 3600 Å*

N.A. Sokolov[1,2,3]

[1] University of Crete, Physics Department, Heraklion 714 09, Crete, Greece
[2] Foundation for Research and Technology - Hellas, P.O. Box 1527, Heraklion 711 10, Crete, Greece
[3] Central Astronomical Observatory at Pulkovo, St. Petersburg 196140, Russia

Received October 18, 1993; accepted November 28, 1994

Abstract. — A method of determination of the effective temperature of B, A and F main sequence stars is proposed, using the slope of the continuum between 3200 Å and 3600 Å. The effective temperature calibration is based on a sample of stars with energy distributions known from UV to the red. We have determined the Balmer jump and the effective temperatures for 235 main sequence stars. The temperatures found have been compared with those derived by Underhill et al. (1979), Kontizas & Theodossiou (1980), Theodossiou (1985), Morossi & Malagnini (1985). The comparison showed good agreement for most of the stars in common. On the other hand, the temperatures derived from the reddening-free colour factor QUV, from the colour index $(m1965-V)$ and from $(B-V)$, given in Gulati et al. (1989), are systematically lower than our temperatures, however the differences are within one-sigma error.

Key words: stars: atmospheres — stars: early-type — stars: fundamental parameters

1. Introduction

Most of our knowledge about stellar atmospheres comes from basic physical parameters for individual stars such as effective temperature (T_{eff}) and surface gravity. Accurate T_{eff} are needed for locating stars on the HR diagram, and for abundance determinations.

In principle, the effective temperature of a star is derived from the integration of flux per unit area of stellar surface on the basis of the spectral energy distribution from the ultraviolet to the infrared. Additionally, we need to know the distance, the angular diameter and the interstellar extinction for the star.

In the visible part of the spectrum numerous tools are available to determine T_{eff}, including the slope of the Paschen continuum or colour photometry, and the Balmer jump in hot stars.

Ultraviolet fluxes are very important for deriving T_{eff} of early-type stars since most of their energy is emitted in this wavelength range, which is inaccessible to ground-based observations. Several calibrations of T_{eff} using visible-ultraviolet (V-UV) colour indices have been published (Malagnini et al. 1984; Lanz 1985; Theodossiou 1985; Gulati et al. 1989). In the last paper the authors have shown that V-UV colour indices depend upon the interstellar extinction law, which in the far-UV region of the spectrum shows variations from region to region of the sky (Meyer & Savage 1981). Unlike the far-UV spectral region, the interstellar extinction law appears to be less variable in the Balmer continuum between 3200 Å and 3600 Å although this spectral region is affected by atmospheric extinction. However, if we use observational data which are very accurately corrected for atmospheric extinction, then we can use the Balmer continuum between 3200 Å and 3600 Å in order to derive the effective temperatures of the stars.

In this paper we will discuss the determination of the effective temperatures of B, A and F main sequence stars, using the slope of the Balmer continuum between 3200 Å and 3600 Å. We will also derive the Balmer jump discontinuity for all of the stars in the sample. This study is based on ground-based observations of the stars measured by Pulkovo astronomers, covering both northern and southern hemispheres (Alekseev et al. 1978; Alekseeva et al. 1992), as described in Sect. 2. The method of determination of the slope in the Balmer continuum and the reduction for interstellar extinction are discussed in Sects. 3 and 4, respectively. The calibration of the slope Φ_{u} vs Θ_{eff} is presented in Sect. 5. The principal results and discussion are presented in Sect. 6.

*Table 3 is also available in electronic form at the CDS via anonymous ftp 130.79.128.5

2. Source of the data

Stars were selected from two catalogues of low-resolution spectra, which were observed by Pulkovo astronomers (Alekseev et al. 1978; Alekseeva et al. 1992). These catalogues archieved at the Pulkovo Observatory on a PC, include the spectra of approximately 500 stars with $V < 6.5^{\rm m}$, in the wavelength region from 3100 Å to 7400 Å with a step of 25 Å for stars of both the northern and the southern hemispheres.

The observations were obtained with the SF-68 spectrophotometer mounted on the AZT-7 telescope, which makes it possible a sensitive control of the instrumental system before and after the observation of each star. The spectra were corrected for atmospheric extinction and transformed into absolute units. The atmospheric extinction was measured every night and the time-dependent curve for every night was found using the Nikonov method (Nikonov & Nikonova 1952) for atmospheric extinction correction. The energy distribution for each star is the mean energy distribution, taken, as a rule, out of 4 – 6 separate observations of the star in different observing sessions. The accuracy of the spectrophotometric catalogues is no worse than 2–3% in the visible region and ~5% in the near-UV (Hagen-Torn & Ruban 1982). The very accurate observational data allowed us to use the wavelength region from 3200 Å to 3600 Å to determine accurately the slope of the continuum for B, A and F main sequence stars as described in the next section.

In the first catalogue (Alekseev et al. 1978) the energy distribution of *Vega* in the absolute flux calibration of Oke & Schild (1970) was used. In the second catalogue (Alekseeva et al. 1992) the energy distribution of *Vega* in the absolute flux calibration by Hayes (1985) was used. To ensure compatibility, we have reduced the energy distribution of all stars to the Hayes (1985) absolute flux calibration. From this resulting data base, we have selected the stars of B, A and F spectral classes, while discarding the following objects:

– supergiants (luminosity classes I and II),
– unresolved double stars with $\Delta V < 4^{\rm m}$,
– variable stars (the criterion was a photometric variation of $\Delta V > 0\overset{\rm m}{.}05$),
– peculiar Am, Ap stars (identified in the General Catalogue of Ap and Am stars by Renson et al. (1991)) and Be stars (identified in the Catalogue of Be stars of Jaschek & Egret 1982).

For each star of our sample we obtained the $E(B-V)$ value using values of $B-V$ taken from the Bright Star Catalogue (Hoffleit & Jaschek 1982) and values of $(B-V)_0$ taken from the tabulation of Straižys (1977). Among the selected stars, we have found stars with negative values of $E(B-V)$. In the following analysis, we decided to include these stars in our study, because the small errors in spectral classification may lead to large errors in $(B-V)_0$, and plus the errors in values of $B-V$ may change the determined value of $E(B-V)$ by as much as 0.03. On the other hand, these stars can have energy distribution different from normal stars in the visible region of the spectrum and same energy distribution in the Balmer continuum near the Balmer jump. For all stars with $E(B-V) < 0.00$, we assume that the observed $(B-V)$ is equal to the intrinsic $(B-V)_0$, so that the colour excesses in these cases are set to zero and the observations are not corrected for interstellar extinction. Stars with $E(B-V) > 0.25$ are excluded.

In the final list we have selected a total of 235 B, A and F main sequence stars. The selected stars are listed in Table 3 together with their spectral class and colour excess $E(B-V)$.

3. Description of the method

In this section we discuss the method used to derive the effective temperatures of the stars by using the slope of the Balmer continuum between 3200 Å and 3600 Å. The actual energy distribution of main sequence stars is influenced by the frequency dependence of the absorption coefficient, which, in the ultraviolet, is mainly due to Balmer hydrogen and metallic continua as well as to metallic lines for stars of the spectral classes A7 - F9. However, the absorption coefficient in the wavelength region from 3200 Å to 3600 Å is not strongly dependent on the frequency. Therefore, the slope of the continuum in the wavelength region from 3200 Å to 3600 Å will be a function of $T_{\rm eff}$ only. To further investigate this idea, we decided to use the extensive grids of stellar models computed by Kurucz (1979), including atomic line blanketing for solar abundance and for metal-rich atmospheres. These models show that the visible colours of the $\log g = 4$ models normalized at 1.8 μm^{-1} can be used to determine $T_{\rm eff}$ from spectrophotometry. As we can see in Fig. 19 of Kurucz (1979), there is a dramatic change with temperature of the slope in the Balmer continuum between 3200 Å and 3600 Å .

Based on this model prediction, as well as on the fact that interstellar extinction law varies slowly from region to region on the sky in this spectral region, we decided to use the slope in this spectral region to determine the effective temperatures of B, A and F main sequence stars. In this region a relative increase of the slope of the Balmer continuum with increasing effective temperature is expected.

In order to determine the slope of the Balmer continuum between 3200 Å and 3600 Å we use the following formula:

$$\Delta m_\lambda = \Psi_{\rm u} + \Phi_{\rm u} \cdot (1/\lambda) \qquad (1)$$

where $\Delta m_\lambda = m_\lambda - m_{5550\rm\AA}$, the parameter $\Phi_{\rm u}$ is the slope of the Balmer continuum and $\Psi_{\rm u}$ is the constant term of the linear approximation, when the label u refers to the

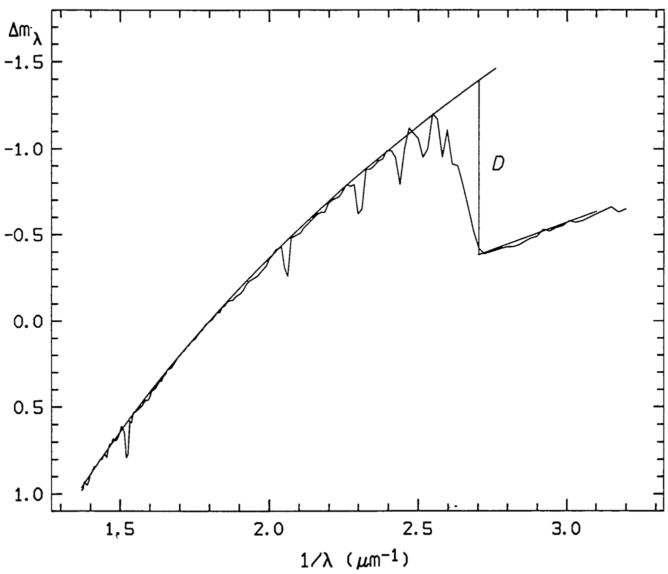

Fig. 1. a) The energy distribution in magnitudes for HR 3982 (sp. B7 V) is plotted, together with the two curves fitted in the Balmer & Paschen continua, respectively. The size of the Balmer jump is shown by a vertical line

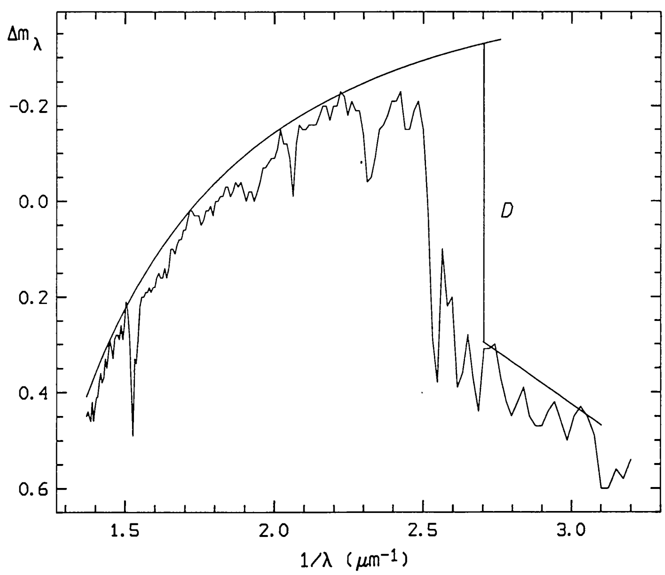

Fig. 1. b) Same as 1a) for HR 5404 (sp: F7 V)

U band. The values of the parameters and related errors (σ_Ψ, σ_Φ) can be found from the least-squares method.

First, the energy distribution of the stars is reduced to absolute units by referring it to the absolute energy calibration of the primary standard star *Vega* by Hayes (1985). Care was taken to use the same absolute calibration of *Vega* for both catalogues from which we draw our sample, since significant systematic differences are known to exist between different such calibrations (Hagen-Torn & Ruban 1982).

For determination of the shape of the continuum at both sides of the Balmer jump, we used an iterative procedure that permits us to exclude absorption lines. For each star, the procedure consists of the following steps:
a) using the least-squares method we compute the values of the parameters of the Balmer continuum (linear approximation) and of the Paschen continuum (a nonlinear approximation of the form $\Delta m_\lambda = \alpha + \beta \cdot \lambda^{-\gamma}$, where α, β and γ are determined from the least-squares fit);
b) compute the deviations of the observational data from the fitted curve and discard all points lying below the fitted curve with deviations bigger than the observational error. These excluded points are never used again;
c) go back to step (a) unless no points were excluded at step (b).

For the majority of our stars of spectral classes B - A, the influence of the absorption lines is negligible and only for stars of spectral classes A7 - F9 the continuum can be seriously affected by the lines. Figure 1 shows the observed energy distribution and the fitted curves of the Balmer and Paschen continuum as a function of wavenumber for the typical case of the star HR 3982 of spectral class B7 V (Fig. 1a) and for the extreme case of the star HR 5404 of spectral class F7 V (Fig. 1b). As we can see for the star HR 3982, the Balmer continuum is not affected by the absorption lines and the Paschen continuum is only partly affected by the Balmer lines. However, for HR 5404 it is very difficult to determine the true continuum at both sides of the Balmer jump, but the shape of the continuum found by the algorithm seems to be quite satisfactory.

The Balmer jump discontinuity is one of the key parameters for stellar spectra of early and intermediate spectral types. Empirical data on this parameter are essential for comparisons with stellar energy distribution data obtained from model atmospheres. Moreover, the Balmer jump is used for stellar classification in a wide variety of photometric and spectrophotomertic classification systems. Using our method, we calculate the size of the Balmer jump, D, by extrapolating the two fitted curves to $\lambda = 3700$ Å. D is defined as:

$$D = \log\left(\frac{F^{3700+}}{F^{3700-}}\right) \qquad (2)$$

where F^{3700-} and F^{3700+} are the fluxes at $\lambda = 3700$ Å of the Balmer continuum and Paschen continuum respectively. The resulting values are given in Cols. 5 of Table 3.

4. Correction for interstellar extinction

Most of the previous determinations of $T_{\rm eff}$ used the mean interstellar extinction curve from the visible to the far-UV spectral regions in order to correct the stellar energy distributions for interstellar extinction (Underhill et al. 1979; Malagnini et al. 1983; Theodossiou 1985). However, this assumption is applicable only to the visible spectral region and not always to the far-UV. Meyer & Savage (1981) have shown that the interstellar extinction law in the far-UV can change from region to region of the sky. They have divided all sky into 12 regions and have computed the average interstellar extinction curve for each region by using the five-band UV photometry for 1347 stars observed by the Astronomical Netherlands Satellite (ANS).

Practically, in the case of the near-UV between 3200 Å and 3600 Å we can only use the mean interstellar extinction curve, because the ANS data have only one point in the spectral region of interest here and therefore we can not determine the slope of the interstellar extinction curve. On the other hand, we can compute the relative errors of the slopes of the interstellar extinction curve from region to region of the sky by averaging the slopes of the 12 regions and deriving the standard deviation from the mean in the far-UV and afterwards extrapolate these errors into the near-UV. In this case we can approximately estimate the possible variance of the slope of the interstellar extinction curve from region to region of the sky in the near-UV. In order to make this estimation, we used the data of Table 3 from Meyer & Savage (1981). So, we calculated the values of the slopes of the interstellar extinction curve S(15-18), S(18-22), S(22-25) and S(25-33) normalized to $E(B-V)=1$ and $\Delta\lambda^{-1}=1$ for each region of the sky using Eq. (3):

$$S(\lambda_1-\lambda_2)=\frac{E(\lambda_1-\lambda_2)}{E(B-V)\Delta\lambda^{-1}} \qquad (3)$$

The values of the mean slope $S(\lambda_1-\lambda_2)$, standard deviation σ_S and relative error $\sigma_{\rm rel}=\sigma_S \,/\, |\, S(\lambda_1-\lambda_2)|$ were calculated by using the values of the slopes for all the 12 regions of the sky, according to the standard propagation theory of errors and are presented in Table 1. From this table we can see that the relative errors change dramatically from the near-UV (5.52%) to the far-UV (53.95%). This fact can also be seen in Fig. 6 of Meyer & Savage (1981) where the normalized curves of the interstellar extinction for stars exhibiting peculiar extinction are given. We have found very good correlation between $\log(\sigma_{\rm rel})$ and wavenumber. A linear regression gives the following relation $\log(\sigma_{\rm rel})=0.389\lambda^{-1}-0.607$, with a linear correlation coefficient of $r=0.941$. This formula was extrapolated to $\lambda=3400$ Å, central wavelength of our spectral region, giving the value of 3.45% for the relative error. Also we can determine the mean slope of the interstellar extinction curve in our spectral region by using the mean interstellar extinction law of Straižys (1977) (in Table 1 marked by *) and find the standard deviation σ_S of the mean slope of the interstellar extinction curve in our spectral region. Our estimate shows that there is a very small variation ($\sigma_S=0.048$) in the slope of the interstellar extinction curve in the spectral region between 3200 Å and 3600 Å in different directions of the sky. This fact allows us to use the mean interstellar extinction law in order to correct the observational slopes of the stellar spectra for interstellar extinction.

Table 1. The slopes of the interstellar extinction curve in the ultraviolet region of spectra (see text)

Name	λ^{-1} (μm^{-1})	$\Delta\lambda^{-1}$ (μm^{-1})	Mean slope	σ_S	$\sigma_{\rm rel}$ (%)
S(15-18)	5.97	0.90	0.443	0.239	53.95
S(18-22)	5.00	1.01	-1.632	0.335	20.53
S(22-25)	4.26	0.53	4.340	0.500	11.52
S(25-33)	3.45	0.98	2.155	0.119	5.52
S(32-36)	2.94	0.35	1.388*	0.048	(3.45)

In order to evaluate the effect of the errors in $E(B-V)$ on the determination of the slope in the Balmer continuum, a preliminary test was performed. This test shows that for stars with small interstellar reddening ($E(B-V)<0.1$) this effect is negligible, and only for stars with $E(B-V)>0.1$ it becomes important. As an example, the observed energy distribution of the star HR 5993 not corrected for reddening together with the reduced data for the three cases with $E(B-V)=0.18$, 0.21 and 0.24 and the adopted interstellar extinction law with $E(B-V)=0.21$ are plotted in Fig. 2. From this figure we can see, that the

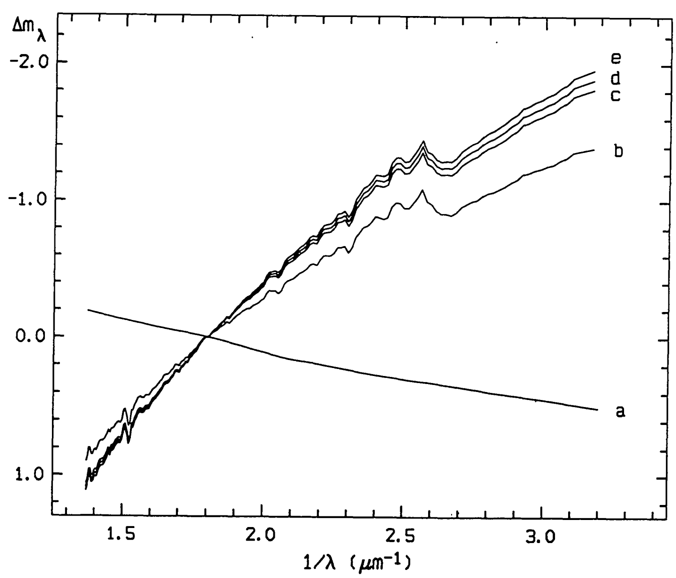

Fig. 2. The energy distribution in magnitudes for the reddened star HR 5993 Sp: B1 V (b) is plotted, together with the adopted interstellar extinction curve (a), and reduced energy distributions corresponding to $E(B-V)$=0.18 (c), $E(B-V)$=0.21 (d), and $E(B-V)$=0.24 (e)

energy distributions for this star show a large variations in the Balmer continuum, while the influence of different values of $E(B-V)$ on the slope in the Balmer continuum is rather small. Anyway, for the stars with high $E(B-V)$

values, we have taken into account the errors, both in the interstellar extinction law ($\sigma_S = 0.048$) and in $E(B-V)$ ($\sigma_E = 0.03$), in calculating the errors in $T_{\rm eff}$ (see Eq. (7)).

All the stars in our sample have small values of $E(B-V)$ and only six stars have $E(B-V) > 0.1$. Since the observational errors in $(B-V)$ and $(B-V)_0$ are almost on the same order as that of $E(B-V)$, zero reddening has been adopted for the stars with $E(B-V) < 0.03$. In the cases when the values of $E(B-V) > 0.03$, we have corrected the energy distribution of the stars for interstellar extinction using the mean interstellar extinction law of Straižys (1977) and the colour excess $E(B-V)$ of the stars.

5. Temperature calibration

5.1. *Selection of temperature standards*

The total flux F emitted by the stellar surface is related to the observed flux f measured outside the earth's atmosphere by

$$F = f\left(\frac{d}{R}\right)^2 = \frac{4f}{\theta^2} \quad (4)$$

(d: distance of the star, R: stellar radius, θ: angular diameter). Once the total flux F is known, the effective temperature $T_{\rm eff}$ can be directly calculated from its definition:

$$T_{\rm eff} = \sqrt[4]{\frac{F}{\sigma}} \quad (5)$$

Hanbury Brown et al. (1974) measured angular diameters θ for 32 stars with an intensity interferometer at the Narrabri Observatory. These measurements were used by Code et al. (1976) and by Beeckmans (1977) to determine $T_{\rm eff}$ from Eqs. (4) and (5) for these stars. This method is known as the direct method (Böhm-Vitense 1981), since the absolute fluxes per unit area of stellar surface are computed using the directly observed apparent angular diameters. This is the best method, since it fits in very well with the definition of effective temperature, but, on the other hand, it has a practical limitation due to the small number of stars for which observed apparent angular diameters are available.

Another method was used by Malagnini et al. (1986) who fitted model spectra to observed spectra by varying $T_{\rm eff}$, g and θ, and derived the temperature from θ and the integrated flux using Eqs. (4) and (5). Since this method uses the full range of the spectra in order to obtain θ, the influence of some wrongly calibrated fluxes is minimized.

In order to determine the angular diameter and effective temperature of stars with unknown diameter, Blackwell & Shallis (1977) developed the infrared flux method (IRFM). The ratio of the total integrated flux to a monochromatic integrated flux, which is only weakly dependent on temperature, is used to determine the angular diameter and effective temperature simultaneously by means of an iterative procedure. A detailed description of this method is given in Remie & Lamers (1982). Though often used (e.g. Blackwell & Shallis 1977; Underhill et al. 1979; Remie & Lamers 1982; Leggett et al. 1986; Mégessier 1988), this method suffers from systematic errors. According to Mégessier (1988), there are two possible sources of error: the employed model fluxes or the infrared calibration.

Based on these considerations, we decided to use only $T_{\rm eff}$ determined by Code at al. (1976) and Malagnini et al. (1986) for the calibration of normal stars, but discarded stars according to the criteria described in the previous section. We also discarded the very fast rotating stars, because the structure of the atmosphere and thus the emerging flux are changed. General data about the stars were taken from the Bright Star Catalogue of Hoffleit & Jaschek (1982). The value $E(B-V)$ was calculated according to the procedure described in Sect. 2. The resulting sample is listed in Table 2.

5.2. *Relationship between $\Theta_{\rm eff}$ and $\Phi_{\rm u}$*

Just as the (V-UV) colour indices, the slope of the energy distribution in the Balmer continuum between 3200 Å and 3600 Å can be a very good indicator of the effective temperature of the stars for a very wide temperature interval and can have a linear relationship with $\Theta_{\rm eff}$=5040/$T_{\rm eff}$. In order to determine the relationship between $\Theta_{\rm eff}$ and $\Phi_{\rm u}$ we have computed the slopes in the Balmer continuum for all stars of Table 2 by using Eq. (1). The resulting values of $\Phi_{\rm u}$ are shown in the last column of Table 2. We also plotted $\Theta_{\rm eff}$ against $\Phi_{\rm u}$ for the reference stars, and derived the linear least squares fit through the data points.

Figure 3 shows this plot, together with the best fitted line. We derived the following linear relationship:

$$\Theta_{\rm eff} = a + b \cdot \Phi_{\rm u} \quad (6)$$

where $a = 0.605 \pm 0.015$

and $b = 0.334 \pm 0.007$

As far as the errors on $T_{\rm eff}(\Phi_{\rm u})$ are concerned, we computed them by taking into account the contributions from different terms, according to the standard propagation theory of errors:

$$\sigma_{T_{\rm eff}} = A \cdot [\sigma_a^2 + \Phi_{\rm u}^2\sigma_b^2 + b^2(\sigma_\Phi^2 + E^2\sigma_S^2 + S^2\sigma_E^2)]^{\frac{1}{2}} \quad (7)$$

where A=${T_{\rm eff}}^2$/5040, σ_a and σ_b refer to the errors in the coefficients of the calibration and σ_Φ is the error in the slope of the energy distribution. The values σ_S and σ_E are equal to 0.048 and 0.03 respectively, and correspond to the errors in the slope S of the mean interstellar extinction law and in the colour excess $E(B-V)$. In the case of stars with $E(B-V) < 0.03$, the energy distribution was not

Table 2. The stars with well known temperatures used as standards taken from Code et al. (1976) and Malagnini et al. (1986). If $T_{\rm eff}$ is given in both sources the mean value is quoted

HR	*Name*	*Sp.type*	V (mag)	$(B-V)$ (mag)	$E(B-V)$ (mag)	$T_{\rm eff}$ (K)	$T_{\rm eff}(\Phi_{\rm u})$ (K)	$\sigma T_{\rm eff}(\Phi_{\rm u})$ (K)	$\Phi_{\rm u}$
269	μ And	A5 V	3.87	+0.13	-0.02	8070	7880	280	0.102
591	α Hyi	F0 V	2.86	+0.28	-0.02	7120	7020	240	0.339
1122	δ Per	B5 III	3.01	-0.13	0.04	13840	13290	930	-0.676
1756	λ Lep	B0.5 IV	4.29	-0.26	0.03	27580	27270	2730	-1.258
1790	γ Ori	B2 III	1.64	-0.22	0.02	21580	21700	1800	-1.116
2421	γ Gem	A0 IV	1.92	+0.00	0.03	9260	8900	290	-0.116
2943	α CMi	F5 IV-V	0.38	+0.42	-0.02	6520	6340	280	0.568
3685	β Car	A2 IV	1.68	+0.00	-0.05	9240	8910	260	-0.117
3775	θ UMa	F6 IV	3.17	+0.46	0.00	6360	6450	310	0.527
3982	α Leo	B7 V	1.35	-0.11	0.01	12210	12540	540	-0.608
4295	β UMa	A1 V	2.37	-0.02	-0.04	9170	9200	300	-0.172
4357	δ Leo	A4 V	2.56	+0.12	0.00	8080	8080	260	0.056
4534	β Leo	A3 V	2.14	+0.08	0.00	8850	8720	300	-0.080
4540	β Vir	F9 V	3.61	+0.55	0.00	6040	6150	300	0.641
5132	ϵ Cen	B1 III	2.30	-0.22	0.03	25740	26450	2560	-1.241
5191	η UMa	B3 V	1.86	-0.19	0.02	16720	17200	1090	-0.934
5264	ρ Vir	A3 V	4.26	+0.10	0.01	8420	8290	240	0.009
5404	θ Boo	F7 V	4.05	+0.50	0.01	6240	6430	290	0.534
5447	σ Boo	F2 V	4.46	+0.36	0.00	6940	7280	270	0.262
6556	α Oph	A5 III	2.08	+0.15	0.00	7970	8040	260	0.066
6879	ϵ Sgr	B9.5 III	1.85	-0.03	0.02	9460	8930	280	-0.120
7001	α Lyr	A0 Va	0.02	+0.00	0.02	9660	9830	320	-0.276
7528	δ Cyg	B9.5 IV	2.87	-0.03	0.02	9880	9820	320	-0.276
7557	α Aql	A7 V	0.76	+0.22	0.02	8010	8040	270	0.065
7790	α Pav	B2 IV	1.94	-0.20	0.02	17880	17560	1240	-0.952
7906	α Del	B9 IV	3.77	-0.06	0.01	10960	11110	400	-0.453
8425	α Gru	B7 IV	1.74	-0.13	-0.02	14050	14860	750	-0.796
8728	α PsA	A3 V	1.16	+0.09	0.00	8670	8900	310	-0.115

corrected for interstellar reddening, so we have taken into account only the errors in the coefficients of the calibration and the error in the slope of the energy distribution.

To test the validity of the calibration obtained, we applied Eq. (6) to the stars of Table 2 and compared the computed temperatures $T_{\rm eff}(\Phi_{\rm u})$ reported in Col. 8 with "standard" values $T_{\rm eff}$ reported in Col. 7. A comparison of the values from Cols. 7 and 8 shows no pronounced systematic discrepancies between them. The correlation coefficient between two sets of data is equal to $r = 0.998$. Therefore, we can use the relationship (6) and (7) for the determination of the effective temperatures and the related errors of B, A and F main sequence stars. We would like to note that for program stars with $T_{\rm eff} > 27000$ K, the calibration curve was extrapolated.

6. Results and discussion

We applied the previously derived calibration to the 235 program stars. Table 3 gives for each star identified by its HR and HD numbers, the spectral class, colour excess $E(B-V)$, Balmer jump, temperature and error obtained from the relationships (2), (6) and (7), respectively.

The values of $T_{\rm eff}$ derived here are compared to the values given by Gulati et al. (1989) for 29 common stars with $T_{\rm eff} > 10000$ K (see Fig. 4). We have also included stars with $T_{\rm eff} > 27000$ K in order to evaluate the influence of the extrapolation of our calibration curve on the determination of the $T_{\rm eff}$ for the hottest stars. In the Gulati et al. (1989) compilation the effective temperatures are derived from the colour factor QUV, colour index $(m1965-V)$ and $(B-V)$. The authors have corrected the far-UV data for interstellar extinction using the interstellar extinction curves of Meyer & Savage (1981) for twelve regions on the sky and have derived twelve calibrations one for each region. In Fig. 4, the circles indicate $T_{\rm eff}$ derived from the colour factor QUV, the crosses indicate $T_{\rm eff}$ derived from the colour index $(m1965-V)$ and squares indicate $T_{\rm eff}$ derived from $(B-V)$ versus $T_{\rm eff}$ derived from $\Phi_{\rm u}$. As we can see from Fig. 4, in most of the cases (with the exception of four stars) $T_{\rm eff}$ derived from $\Phi_{\rm u}$ are systematically higher than $T_{\rm eff}(QUV)$, $T_{\rm eff}(m1965\text{-}V)$ and $T_{\rm eff}(B-V)$, by about 1630 K, 1490 K and 1390 K, respectively. This discrepancy cannot be the result of systematic errors in the correction of the slopes for interstellar reddening, because most of the common stars are unreddened stars. So, we have one star with $E(B-V) = 0.12$, eight stars with $0.05 < E(B-V) < 0.12$ and twenty stars with $E(B-V) < 0.05$. On the other hand, the discrepancy is present in both the far-UV colour indices and the visible

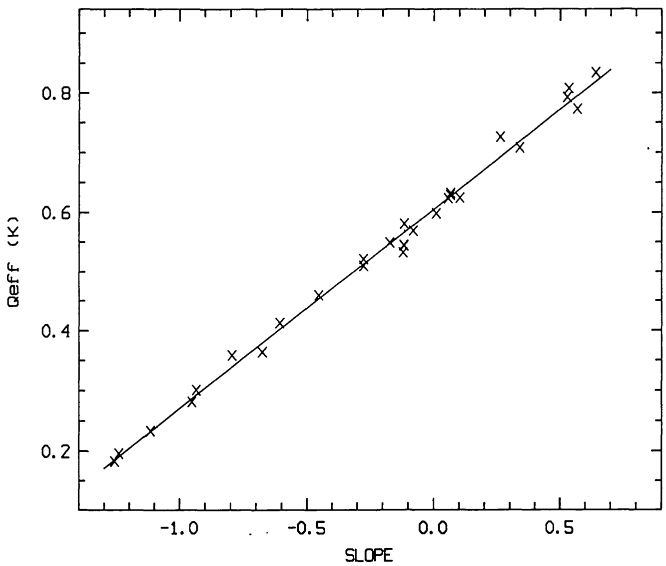

Fig. 3. Temperature calibration. Correlation between $\Theta_{\rm eff} = 5040/T_{\rm eff}$ and the slope of the energy distribution from 3200 Å to 3600 Å

colour index $(B-V)$ for which the mean interstellar law is more reliable. Most likely the discrepancy is due to the calibration of the colour indices in the work of Gulati et al. (1989) or to our calibration of the slope in the Balmer continuum. Gulati et al. (1989) used 120 stars as reference stars for which $T_{\rm eff}$ have been determined by either direct, semidirect or indirect methods in order to establish the $T_{\rm eff}$ calibrations of suitable colours and/or colour factor. Moreover, the authors used both main sequence stars and supergiant stars. It should be noted that for the early-type B supergiants there are systematical disagreement between $T_{\rm eff}$ derived from the integration of the spectral energy distribution and $T_{\rm eff}$ derived from the analysis of the relative strengths of temperature-sensitive lines of the same element. Underhill et al. (1979) suggested that the large differece between the high values of $T_{\rm eff}$ derived from the line spectrum and the low $T_{\rm eff}$ derived from the integrated flux, is due to the fact that the lines are formed in the hotter chromospheric region. Furthermore, Remie & Lamers (1982) have suggested that the discrepancy might be due to the blanceting by the far UV lines in the stellar wind of the supergiants. In the present work we obtained the linear relationship between $T_{\rm eff}$ and the slope of the Balmer continuum by using only "normal" main sequence stars.

To check our calibration, we have compared the temperatures derived from $\Phi_{\rm u}$ with those obtained by Underhill et al. (1979), Kontizas & Theodossiou (1980), Theodossiou (1985), Morossi & Malagnini (1985). Underhill et al. (1979) used the infrared flux method and Kontizas & Theodossiou (1980) and Theodossiou (1985) compared the observed ultraviolet and visual energy distributions with the grid of the model atmospheres of Kurucz (1979), using an approach very similar to that of Morossi & Malagnini (1985).

The agreement between $T_{\rm eff}(\Phi_{\rm u})$ and $T_{\rm eff}$(UDPD), obtained by Underhill et al. (1979), for the 49 hot stars in common appears to be very good, as illustrated in Fig. 5 and is confirmed by the following results: the mean difference between the two sets of data $\Delta T_{\rm eff} = 42$ K, with a linear correlation coefficient $r = 0.970$, and $\alpha = 1.067$ for the slope of the regression line of $T_{\rm eff}(\Phi_{\rm u})$ vs. $T_{\rm eff}$(UDPD).

For the subset of 64 stars in common with the data from Kontizas & Theodossiou (1980) and Theodossiou (1985), good agreement is also found between $T_{\rm eff}(\Phi_{\rm u})$ and $T_{\rm eff}$(KT&T) ($\Delta T_{\rm eff} = 134$ K, $r = 0.990$, $\alpha = 1.007$), as shown in Fig. 6.

In addition, we have compared the $T_{\rm eff}(\Phi_{\rm u})$ with $T_{\rm eff}$(MM) from the work by Morossi & Malagnini (1985) for 83 common stars. A comparison gives the following results: $\Delta T_{\rm eff} = 353$ K, $r = 0.984$, $\alpha = 0.941$ and the plot of $T_{\rm eff}(\Phi_{\rm u})$ versus $T_{\rm eff}$(MM) is given in Fig. 7. We have not taken into account the fact that for some stars Underhill et al. (1979) and Kontizas & Theodossiou (1980), Theodossiou (1985) have adopted a log g value different from those used by Morossi & Malagnini (1985) as reported in their Table 2.

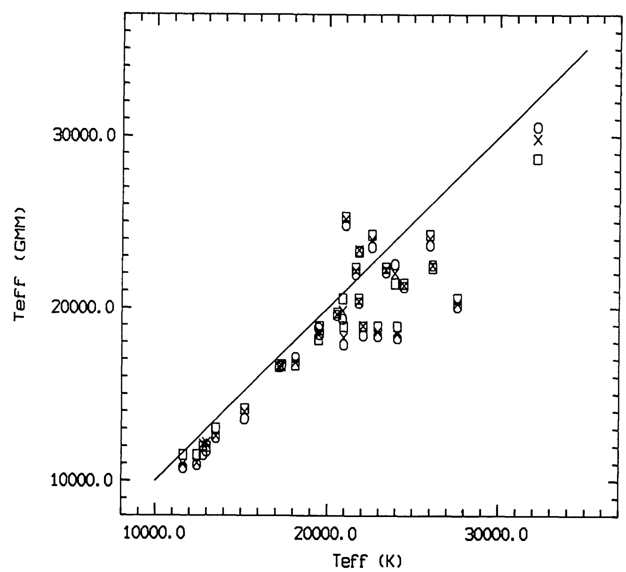

Fig. 4. Comparison of $T_{\rm eff}$ derived by Gulati et al. (1989) from QUV (circles), $(m1965-V)$ (crosses) and $(B-V)$ (squares) with $T_{\rm eff}$ derived in this work

Generally, there are no significant differences between the temperatures derived from $\Phi_{\rm u}$ and the temperatures derived from fluxes by other authors. The agreement between $T_{\rm eff}(\Phi_{\rm u})$ and $T_{\rm eff}$ derived from different sources for stars with $T_{\rm eff} > 27000$ K is also good, thus supporting the reliability of the extrapolation of the calibration curve. The difference between the temperatures derived in Gulati

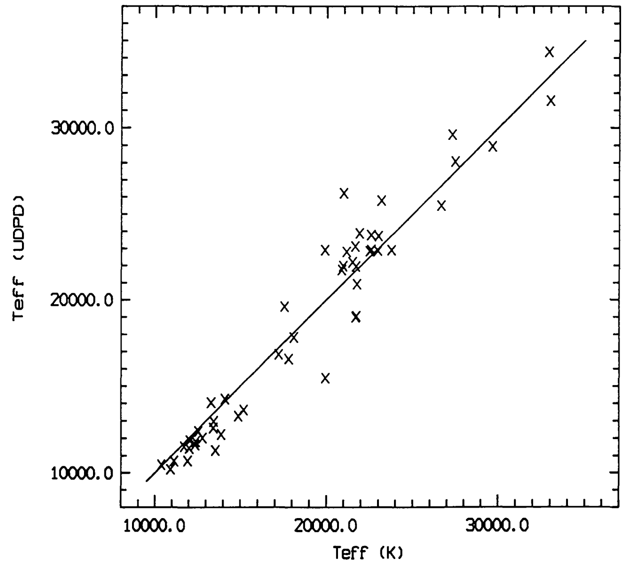

Fig. 5. Comparison of $T_{\rm eff}$(UDPD) derived by Underhill et al. (1979) with $T_{\rm eff}$ derived in this work

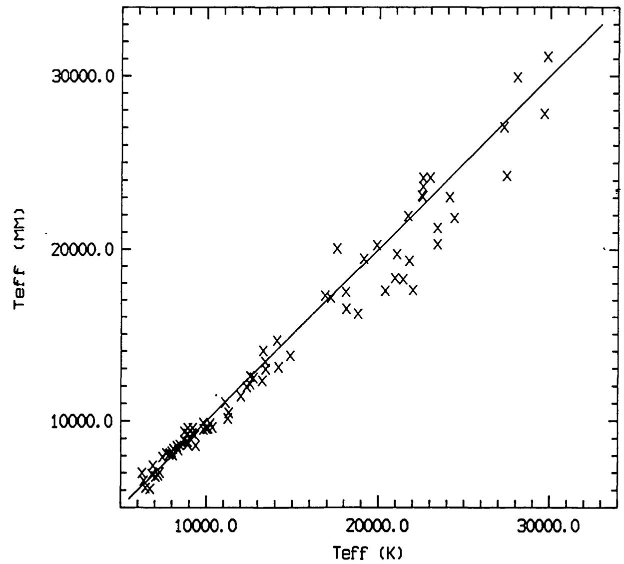

Fig. 7. Comparison of $T_{\rm eff}$(MM) derived by Morossi & Malagnini (1985) with $T_{\rm eff}$ derived in this work

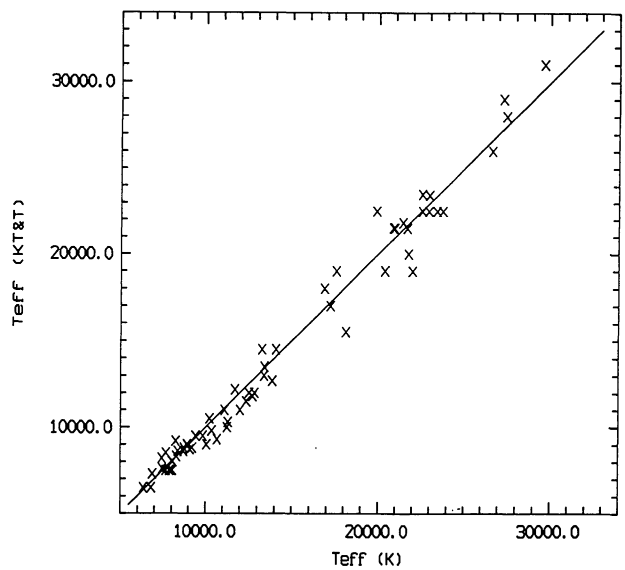

Fig. 6. Comparison of $T_{\rm eff}$(KT&T) derived by Kontizas & Theodossiou (1980) and Theodossiou (1985) with $T_{\rm eff}$ derived in this work

et al. (1989) and the temperatures derived in the present work is, most likely, due to the fact that the authors have used two different sets of data in order to establish the $T_{\rm eff}$ calibrations. On the other hand, if we take into account the errors on temperatures as given by Gulati et al. (1989) and in the present work, then the disagreement between the two sets of data is no more than one sigma error.

Taking into account the observational uncertainties of the slope, the calibration errors, as well as the errors in the mean interstellar extinction law and in the values $E(B-V)$, we have calculated the error of $T_{\rm eff}$ for each star of the our sample. The statistical errors of the temperature determination range from 4% for stars with $T_{\rm eff} \lesssim 10000$ K up to 10% for stars with $T_{\rm eff} \gtrsim 20000$ K.

In our study we have used only normal main sequence stars, but this method can be extended to other kinds of stars. For example, Stepien & Dominiczak (1989) have shown that the energy distribution of Ap stars and the normal main sequence stars in the Balmer continuum near the Balmer jump (at least the slope) is similar (see Fig. 2 of Stepien & Dominiczak 1989). In this way, probably, our method can be applied directly to Ap stars, using a temperature calibration based on main sequence stars.

7. Conclusions

The present study shows that the slope of the Balmer continuum between 3200 Å and 3600 Å can be a very good estimator of $T_{\rm eff}$ for B, A and F main sequence stars. We have determined the $T_{\rm eff}$ for 235 B, A and F main sequence stars from the continuum between 3200 Å and 3600 Å by using the very accurate energy distribution of the stars measured by Pulkovo astronomers. Reliable results can be expected for 6000 K $\lesssim T_{\rm eff} \lesssim$ 27000 K. In the case of the hottest stars with $T_{\rm eff} >$ 27000 K the method is applicable, but the temperatures are less reliable.

From comparison of our $T_{\rm eff}$ with the $T_{\rm eff}$ derived with different approaches and from different sets of observations we concluded that there is good agreement between the $T_{\rm eff}$ for the subsets of the stars in common, except for the case of Gulati et al. (1989) determinations.

In conclusion we state that the slope of the Balmer continuum determined between 3200 Å and 3600 Å is a useful tool for the determination of $T_{\rm eff}$, with statistical errors comparable to those reported for others more costly methods.

Acknowledgements. The author wish to thank Drs. V.A. Hagen-Torn, I.M. Kopylov and E.V. Ruban for their helpful comments. The author particularly wishes to acknowledge the very friendly and thorough discussions that he had with Drs. E. Paleologou and D. Hatzidimitriou. Also I would like to thank the Foundation for Research and Technology - Hellas for the use of their facilities. This work has been partly supported by an American Astronomical Society grant.

References

Alekseev N.L., Alekseeva G.A., Arkharov A.A. et al. 1978, Tr. Gl. Astron. Obs. Akad. Nauk. USSR 83, 4
Alekseeva G.A., Arkharov A.A., Belaev Y.A. et al. 1992, Preprint Vses. Inst. Nauchn. Tekn. Inform. 2113, 96
Beeckmans F. 1977, A&A 60, 1
Blackwell D.E., Shallis M.J. 1977, MNRAS 180, 177
Böhm-Vitense E., 1981, ARA&A 19, 295
Code A.D., Davis J., Bless R.C., Hanbury Brown R. 1976, ApJ 203, 417
Gulati R.K., Malagnini M.L., Morossi C. 1989, A&AS 80, 73
Hagen-Torn E.I., Ruban E.V. 1982, SvA 26, 209
Hanbury Brown R., Davis J., Allen L.R. 1974, MNRAS 167, 121
Hayes D.S. 1979, Dudley Obs. Rep. 14, 297
Hayes D.S. 1985, Stellar Absolute Fluxes and Energy Distribution from 0.32 to 4.0 μm, eds. D.S. Hayes, L.E. Pasinetti, A.G. Davis Philip, IAU Symp. 111, Calibration of Fundamental Stellar Quantities (Reidel, Dordrecht) 225
Hoffleit D., Jaschek C. 1982, The Bright Star Catalogue, Yale University Observatory, New Haven
Jaschek M., Egret D. 1982, Catalogue of Stellar Groups, Sp. Publ. CDS 4, Obs. Strasbourg
Kontizas E., Theodossiou E. 1980, MNRAS 192, 745
Kurucz R.L. 1979, ApJS 40, 1
Lanz T. 1985, A&A 144, 191
Leggett S.K., Mountain C.M., Selby M.J. et al. 1986, A&A 159, 217
Malagnini M.L., Faraggiana R., Morossi C. 1983, A&A 128, 375
Malagnini M.L., Faraggiana R., Morossi C. 1984, in "The MK Process and Stellar Classification", ed. R.F. Garrison (David Dunlap Obs., Toronto, Canada) 321
Malagnini M.L., Morossi C., Rossi L., Kurucz R.L. 1986, A&A 162, 140
Mégessier C. 1988, A&AS 72, 551
Meyer D.M., Savage B.D. 1981, ApJ 248, 545
Morossi C., Malagnini M.L. 1985, A&AS 60, 365
Nikonov V.B., Nikonova E.K. 1952, Izv. Krim. Astrofiz. Obs. 9, 41
Oke J.B., Schild R.E. 1970, ApJ 161, 1015
Renson P., Gerbaldi M., Catalano F.A. 1991, A&AS 89, 429
Remie H., Lamers H.J.G.L.M. 1982, A&A 105, 85
Stepien K., Dominiczak R. 1989, A&A 219, 197
Straižys V. 1977, Multicolor Stellar Photometry, Mokslas, Vilnius
Theodossiou E. 1985, MNRAS 214, 327
Underhill A.B., Divan L., Prévot-Burnichon M.L., Doazan V. 1979, MNRAS 189, 601

Table 3. Balmer jumps, the effective temperatures and their errors for the 235 program stars

HR	*HD*	*Sp.Type*	$E(B-V)$ (mag)	D (dex)	$T_{\rm eff}$ (K)	$\sigma T_{\rm eff}$ (K)
21	432	F2 III-IV	-0.01	0.425	6810	270
26	560	B9 V	0.00	0.441	12420	610
63	1280	A2 V	0.01	0.556	8720	270
100	2262	A7 V	-0.03	0.512	7670	240
114	2628	A7 III	0.04	0.462	7690	350
197	4247	F1 III-IV	0.01	0.322	7400	280
220	4622	B9 V	0.01	0.502	11330	470
269	5448	A5 V	-0.02	0.559	7880	280
403	8538	A5 III-IV	-0.02	0.565	8090	330
520	10939	A1 V	0.02	0.565	10090	370
553	11636	A5 V	-0.02	0.524	8250	300
569	11973	F0 V	-0.02	0.418	7110	310
580	12216	A1 V	-0.03	0.577	9410	290
591	12311	F0 V	-0.02	0.456	7020	240
623	13174	F2 III	-0.01	0.447	6430	230
669	14191	A1 V	-0.01	0.565	10010	360
674	14228	B8 IV-V	-0.02	0.371	14180	670
718	15318	B9 III	0.01	0.511	11300	430
789	16754	A2 V	0.01	0.535	9180	290
804	16970	A3 V	0.00	0.537	8360	240
890	18537	B7 V	0.08	0.364	12910	850
963	20010	F8 V	0.00	0.249	6110	240
1038	21364	B9 V	-0.02	0.386	12730	580
1122	22928	B5 III	0.04	0.333	13290	930
1338	27290	F0 V	0.01	0.369	7180	300
1380	27819	A7 V	-0.05	0.525	7840	290
1394	28052	F0 V	-0.05	0.496	7170	360
1412	28319	A7 III	-0.02	0.530	7690	320
1444	28910	A8 V	0.02	0.462	7730	330
1473	29388	A6 V	-0.06	0.555	7990	290
1479	29488	A5 V	0.00	0.551	8540	340
1617	32249	B3 V	0.02	0.196	21730	1900
1621	32309	B9.5 V	0.00	0.476	10910	420
1666	33111	A3 III	0.05	0.561	8710	380
1679	33328	B2 IV	0.03	0.115	23750	2250
1696	33802	B8 V	0.00	0.347	12050	550
1705	33949	B9 V	-0.03	0.383	12980	570
1735	34503	B5 III	0.05	0.315	14090	870
1756	34816	B0.5 IV	0.03	0.074	27280	2730
1762	34968	A0 V	-0.03	0.522	10720	440
1765	35039	B2 IV-V	0.08	0.169	21520	2190
1770	35149	B1 V	0.12	0.121	24190	2800
1790	35468	B2 III	0.02	0.166	21700	1800
1791	35497	B7 III	-0.01	0.341	13410	610
1810	35708	B2.5 IV	0.07	0.180	21050	2170
1811	35715	B2 IV	0.03	0.114	24130	2060
1839	36267	B5 V	0.02	0.288	18120	1280
1855	36512	B0 V	0.05	0.042	32900	5200
1876	36822	B0 III	0.14	0.069	29840	4270
1892	37018	B1 V	0.08	0.104	27700	3560
1899	37043	O9 III	0.07	0.057	32200	5050
1928	37438	B3 IV	0.05	0.208	22940	2740
1931	37468	O9.5 V	0.07	0.070	33000	5000
1937	37507	A4 V	0.01	0.549	8760	360
1946	37711	B3 IV	0.07	0.238	19470	1830
1952	37756	B2 IV-V	0.04	0.155	23940	2920
1956	37795	B7 IV	0.01	0.345	13870	630
1983	38393	F6 V	0.00	0.264	7220	320
1996	38666	O9.5 V	0.05	0.046	32700	5100
1998	38678	A3 V	0.01	0.535	9080	290
2020	39060	A5 V	0.02	0.490	8230	350
2056	39764	B5 V	0.02	0.285	16930	1040
2085	40136	F1 III	0.02	0.360	7210	310
2088	40183	A2 IV	-0.02	0.557	8340	260
2106	40494	B2.5 IV	0.04	0.248	16870	1300
2128	40967	B5 III	0.04	0.245	17790	1470
2155	41695	A1 V	0.02	0.554	9800	380
2244	43445	B9 V	-0.01	0.468	11920	470
2282	44402	B2.5 V	0.04	0.228	20950	1980
2361	45813	B4 V	0.02	0.257	18800	1330
2421	47105	A0 IV	0.03	0.601	8900	290
2451	47670	B8 III	-0.01	0.384	12350	560
2484	48737	F5 III	0.00	0.318	6420	260
2550	50241	A7 IV	0.01	0.507	7440	240
2571	50707	B1 IV	0.03	0.098	26650	2690
2619	52092	B3 V	0.05	0.245	19530	1880
2845	58715	B8 V	0.01	0.446	11710	490
2922	60863	B8 V	-0.01	0.359	14790	820
2943	61421	F5 IV-V	-0.02	0.317	6340	280
2944	61429	B8 IV	-0.01	0.387	13270	630
2961	61831	B2.5 V	0.04	0.234	22480	2320
3116	65551	B2.5 IV	0.05	0.221	20940	2060
3159	66591	B3 V	0.04	0.128	24090	2830
3192	67797	B5 IV	0.02	0.270	19930	1490
3204	68217	B2 IV-V	0.06	0.194	22080	2450
3240	69081	B1.5 IV	0.07	0.137	24680	2860
3270	70060	A7 III	0.02	0.475	7930	370
3283	70556	B2 IV-V	0.06	0.174	26150	3390
3314	71155	A0 V	0.00	0.533	9910	340
3330	71510	B2 V	0.09	0.231	23210	2610
3442	74146	B4 IV	0.05	0.275	18110	1510
3447	74195	B3 IV	0.02	0.246	16500	1010
3457	74375	B1.5 III	0.12	0.132	27600	3630
3467	74560	B3 IV	0.03	0.244	21430	1900
3468	74575	B1.5 III	0.08	0.123	22990	2380
3476	74753	B0 III	0.01	0.060	29660	3330
3485	74956	A1 V	0.02	0.567	9320	290
3574	76805	B5 V	0.05	0.312	17330	1340
3659	79351	B2 IV-V	0.06	0.219	20880	2040
3685	80007	A2 IV	-0.05	0.609	8910	260
3734	81188	B2 IV-V	0.07	0.195	22120	2250
3753	81848	B6 V	0.04	0.305	19130	1950
3775	82328	F6 IV	0.00	0.320	6450	310
3856	83944	B9 IV-V	0.00	0.450	11620	510

Table 3. continued

HR	*HD*	*Sp.Type*	$E(B-V)$ (mag)	*D* (dex)	T_{eff} (K)	σT_{eff} (K)
3982	87901	B7 V	0.01	0.402	12540	540
4023	88955	A2 V	0.00	0.555	8890	280
4102	90589	F2 IV	0.00	0.307	7320	260
4295	95418	A1 V	-0.04	0.565	9200	300
4357	97603	A4 V	0.00	0.546	8080	260
4390	98718	B5 V	0.03	0.256	15190	1220
4467	100841	B9 III	0.03	0.531	10370	350
4520	102249	A7 III	-0.04	0.554	7870	260
4534	102647	A3 V	0.00	0.536	8720	300
4537	102776	B3 V	0.06	0.237	19620	1880
4540	102870	F9 V	0.00	0.288	6150	300
4549	103079	B4 V	0.08	0.277	20560	2020
4554	103287	A0 V	0.02	0.575	9390	320
4603	104841	B2 IV	0.16	0.223	25700	3430
4638	105937	B3 V	0.06	0.259	20380	1840
4656	106490	B2 IV	0.01	0.137	22570	1840
4679	106983	B2.5 V	0.06	0.217	22820	2460
4689	107259	A2 IV	-0.03	0.569	9370	360
4743	108483	B2 V	0.06	0.185	22350	2330
4757	108767	B9.5 V	0.00	0.508	10350	340
4798	109668	B2 IV-V	0.05	0.160	21900	2170
4802	109787	A2 V	0.00	0.553	8560	230
4819	110304	A1 IV	-0.03	0.577	9330	280
4844	110879	B2.5 V	0.05	0.205	21640	2090
4848	110956	B3 V	0.04	0.248	22000	2440
4853	111123	B0.5 III	0.06	0.093	26650	3270
4897	112078	B4 V	0.04	0.264	19730	1830
4898	112092	B2 IV-V	0.06	0.187	24410	3160
4993	114911	B8 V	0.02	0.380	16130	960
5028	115892	A2 V	-0.01	0.553	9030	290
5035	116087	B3 V	0.08	0.257	23970	3080
5107	118098	A3 V	0.02	0.513	8280	230
5132	118716	B1 III	0.03	0.130	26450	2560
5168	119756	F3 IV	0.00	0.304	7080	270
5185	120136	F6 IV	0.02	0.303	6640	370
5190	120307	B2 IV	0.03	0.138	22570	1810
5191	120315	B3 V	0.02	0.255	17200	1090
5216	120874	A3 V	0.00	0.522	8840	270
5221	120955	B4 IV	0.05	0.285	17910	1460
5231	121263	B2.5 IV	0.00	0.143	21030	1600
5248	121743	B2 IV	0.03	0.170	22540	1840
5249	121790	B2 IV-V	0.05	0.176	21820	2200
5264	122408	A3 V	0.01	0.592	8290	240
5267	122451	B1 III	0.04	0.108	26720	3260
5285	122980	B2 V	0.04	0.179	23410	2740
5354	125238	B2.5 IV	0.04	0.216	19900	1770
5367	125473	A0 IV	-0.01	0.523	10530	390
5404	126660	F7 V	0.01	0.269	6430	290
5425	127381	B2 III	0.05	0.134	25980	3250
5447	128167	F2 V	0.00	0.305	7280	270
5469	129056	B1.5 III-V	0.06	0.136	21820	2160
5471	129116	B3 V	0.04	0.208	24480	2990
5487	129502	F2 III	0.04	0.314	6820	240
5511	130109	A0 V	0.01	0.546	10110	340
5576	132200	B2 IV	0.05	0.177	19890	1830
5685	135742	B8 V	-0.01	0.410	13250	660
5695	136298	B1.5 IV	0.04	0.112	20990	2000
5708	136504	B2 IV-V	0.07	0.204	23410	2510
5776	138690	B2 IV	0.04	0.170	22210	2210
5793	139006	A0 V	0.00	0.554	9860	330
5812	139365	B2.5 V	0.04	0.223	21770	2140
5881	141513	A0 V	-0.02	0.504	10440	400
5897	141891	F2 III	-0.05	0.401	7050	230
5928	142669	B2 IV-V	0.05	0.170	21150	2010
5948	143118	B2.5 IV	0.00	0.157	21490	1630
5953	143275	B0.3 IV	0.17	0.101	29640	4310
5986	144284	F8 IV	-0.01	0.300	6120	320
5993	144470	B1 V	0.21	0.111	27460	3480
6165	149438	B0 V	0.06	0.072	28060	3620
6252	151985	B2 IV	0.03	0.137	21650	1730
6378	155125	A2 V	0.01	0.566	8740	310
6396	155763	B6 III	0.02	0.368	13430	650
6436	156729	A2 V	0.00	0.540	8860	390
6446	156928	A2 V	-0.02	0.593	9130	760
6453	157056	B2 IV	0.03	0.154	22950	1860
6500	158094	B8 V	0.00	0.417	12790	560
6508	158408	B2 IV	0.02	0.164	22490	1840
6537	159217	A0 V	-0.01	0.547	9780	360
6556	159561	A5 III	0.00	0.530	8040	260
6561	159876	F0 IV	-0.03	0.456	6950	260
6580	160578	B1.5 III	0.04	0.132	23170	2400
6588	160762	B3 IV	0.03	0.238	18090	1190
6629	161868	A0 V	0.06	0.568	10340	480
6789	166205	A1 V	0.00	0.572	9070	270
6879	169022	B9.5 III	0.02	0.549	8930	280
7001	172167	A0 Va	0.02	0.584	9830	320
7039	173300	B8 III	-0.01	0.395	12550	520
7069	173880	A5 III	-0.02	0.507	8070	290
7121	175191	B2.5 V	0.01	0.217	21680	1980
7236	177756	B9 V	-0.02	0.455	12010	480
7337	181454	B9 V	-0.03	0.414	13630	660
7340	181577	F0 IV-V	-0.08	0.511	8230	390
7348	181869	B8 V	0.00	0.410	12370	500
7371	182564	A2 III	-0.02	0.576	8420	410
7377	182640	F3 IV	-0.06	0.403	6880	240
7469	185395	F4 V	-0.03	0.289	7180	290
7528	186882	B9.5 IV	0.02	0.525	9820	320
7546	187362	A3 V	0.01	0.531	8320	440
7557	187642	A7 V	0.02	0.470	8040	270
7560	187691	F8 V	0.02	0.284	6360	360
7590	188228	A0 V	-0.01	0.521	11230	430
7710	191692	B9.5 III	-0.02	0.524	11250	430
7790	193924	B2 IV	0.02	0.215	17560	1240
7848	195627	F1 III	-0.03	0.401	7230	330

Table 3. continued

HR	*HD*	*Sp.Type*	$E(B-V)$ (mag)	*D* (dex)	$T_{\rm eff}$ (K)	$\sigma T_{\rm eff}$ (K)
7852	195810	B6 III	0.01	0.325	15190	820
7882	196524	F5 IV	0.01	0.314	6240	270
7906	196867	B9 IV	0.01	0.481	11110	400
7913	197051	A7 III	-0.04	0.577	8300	300
7950	198001	A1 V	-0.02	0.593	9320	300
8001	199081	B5 V	0.03	0.288	17190	1230
8028	199629	A1 V	0.00	0.571	9890	440
8162	203280	A7 V	0.02	0.482	7460	270
8351	207958	F1 III	0.06	0.312	7600	350
8353	207971	B8 III	-0.02	0.392	12380	510
8418	209819	B9 IV-V	0.00	0.409	13530	630
8425	209952	B7 IV	-0.02	0.347	14860	750
8431	210049	A2 V	0.00	0.558	8640	260
8494	211336	F0 IV	-0.01	0.450	7220	260
8518	212061	A0 V	-0.03	0.525	10650	350
8628	214748	B8 V	-0.01	0.395	12840	550
8641	214994	A1 IV	-0.03	0.558	10050	410
8663	215573	B6 IV	0.00	0.312	16440	990
8665	215648	F6 III-IV	0.03	0.252	6730	330
8675	215789	A3 V	-0.01	0.561	7900	210
8695	216336	A0 III	-0.02	0.495	10600	410
8709	216627	A3 V	-0.04	0.585	8450	270
8717	216735	A1 V	-0.02	0.552	9980	440
8728	216956	A3 V	0.00	0.546	8900	310
8781	218045	B9 V	0.03	0.567	10220	340
8848	219571	F1 III	0.09	0.333	7600	300
8976	222439	B9 IV	-0.01	0.461	12030	520